Real-time heat capacity measurement during thin-film deposition by scanning nanocalorimetry

M. Zhang, M. Yu. Efremov, E. A. Olson, Z. S. Zhang, and L. H. Allen[a)]
Department of Material Science and Engineering and Coordinated Science Laboratory, University of Illinois at Urbana-Champaign, Urbana, Illinois 61801

(Received 25 July 2002; accepted 18 September 2002)

The scanning nanocalorimetry technique is utilized to characterize thin-film growth in real-time. The technique generates three-dimensional heat capacity data as a function of temperature and thickness that show the continuous change of indium film during deposition. The measurement interval is $\sim 4\times 10^{-3}$ nm in thickness. Indium thin films form nanoparticles on silicon nitride surfaces that show the phenomena of melting point depression and the formation of magic number size particles. The measured increment of the heat capacity ΔC_p is ~30 pJ/K and the temperature resolution is better than 0.5 K. © *2002 American Institute of Physics.* [DOI: 10.1063/1.1520714]

In situ and real-time measurement techniques are of great importance in thin film studies for microelectronics.[1–3] *In situ* experiments such as x-ray diffraction[4–6] and ellipsometry[7,8] provide contamination-free measurements which can be critical for thin film and surface investigations. Real-time measurements allow the worker to study the evolution of a thin film on an incremental level less than 1 ML. They are suitable to track key aspects of the growth process. The techniques reduce systematic errors which are inherent in ''one-at-a-time'' type experiments. They can lead to the discovery of small effects, which are otherwise submerged by the experimental uncertainties. The fine-scale sampling property also allows one to track processes and effects observable only in narrow thickness ranges.

Heat capacity measurements are useful in characterizing materials. The measurements can be used to study phase transitions such as melting, glass transitions, etc., and to track exothermic/endothermic chemical reactions. Nanocalorimetry[9] technique is especially suitable for measuring the heat capacity of small materials. It is sensitive to measure thin films from submonolayer thick to hundreds of nanometers. Besides the high sensitivity, scanning nanocalorimetry also features adjustable heating rates up to 10^6 K/s. Ultrafast heating allows individual caloric measurement to be performed sequentially within 1 s intervals, thus enabling the characterization of thin film growth in real time.

In this letter, we present real-time scanning nanocalorimetry results on indium deposition. The experiment demonstrates the unusual properties of nanometer sized particles such as melting point depression and magic number sized particles.

Nanocalorimetry is based on specially designed calorimetric sensors made on (100) Si wafers using microfabrication techniques for MEMS devices. Such sensors consist of an extremely thin (30 nm) amorphous silicon nitride membrane mechanically supported by a (0.25 mm thick) silicon frame. A 50 nm thick metal strip is patterned on the topside of the membrane. This metal strip functions as both microheater and a resistive thermometer. To obtain stability, the sensors are first annealed and then calibrated against temperature in a three-zone vacuum tube furnace. The differential concept of calorimetric measurements is employed by using two sensors in one working assembly, one sensor as a sample cell and the other as the reference. Details on calorimeter sensor fabrication and nanocalorimetric measurements can be seen elsewhere.[10]

An indium thin film is deposited onto the nitride side of the sample sensor. The area is about 2 mm^2 aligned to the heater by a shadow mask. The pressure during the entire experiment is maintained at $1-2\times 10^{-8}$ Torr. The calorimetric measurements are initiated by applying synchronized dc electrical pulses to both sample and reference heaters. High heating rates from 30 to 200 k K/s are used to achieve near-adiabatic conditions. The current and voltage through the sensors are measured during the experiment, and are used to calculate resistance and power in the first step, and the temperature and heat capacity in a second step.

The required stability of electrical characteristics of sensors is achieved by annealing at 450 °C under high vacuum ($\sim 10^{-8}$ Torr) for 2 h and by making several thousands repetitive measurements before the experiment. The ''burned-in'' sensors are then electrically stable during the measurement. Indium deposition is accomplished via thermal evaporation. A critical step in this experiment was to replace the inherently noisy silicon control rectifier (SCR) unit by an autotransformer to control the current for evaporation. Small, thin boats are employed to reduce the total power needed for evaporation. This limits the effect of radiation, which ensures that sensor characteristics are stable during the measurement. For the purpose of real-time measurement, a slow, constant evaporation rate (0.24 Å/min) is first achieved. Nanocalorimetry measurements are then taken at 1 s intervals and are averaged every ten scans. Since radiation from the evaporation source causes a shift when the caloric sensor is first exposed to it, a baseline measurement with the radiation effect is used, and caloric measurements before and after the real-time measurement are taken for calibration. The deposited thin film thicknesses are also monitored by a quartz monitor for comparison. Note, the nature of the measurement unavoidably heats the sample—nanocalorimetry scan heats the indium up to 300 °C. The studied thin film is inherently annealed.

[a)]Electronic mail: l-allen9@uiuc.edu

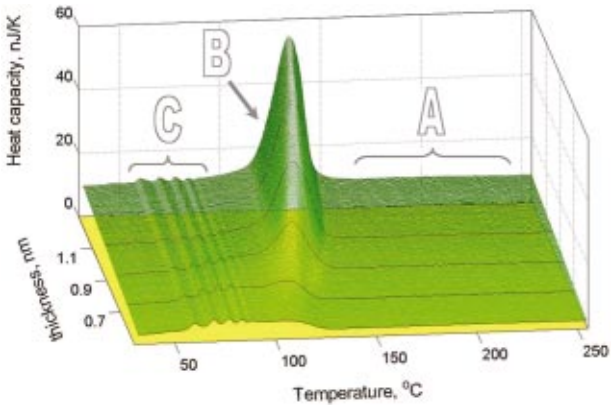

FIG. 1. (Color) 3D plot of heat capacity vs. temperature vs. thickness during the vapor deposition of indium. The plot is generated using sequential individual scans with a heating rate of 30k K/s taken at 1 s intervals. The film is discontinuous and consists of indium nanoparticles. Three distinct features of the plot are: (a) the liquid region which is used to track the growing of thin film on the sub-angstrom scale, (b) the main melting peak of the film which illustrates size-dependent melting, and (c) the multiple maxima, constant in temperature and related to magic number nanoparticles.

Figure 1 shows a 3D plot of heat capacity versus temperature versus thickness that is the result of real-time *in situ* nanocalorimetry. The growth of indium on the silicon nitride surface film follows Volmer–Weber growth dynamics.[11] At the early growth stage, the film is discontinuous and consists of nanometer-sized particles. The particles melt at different temperatures. The melting temperature depends on the surface curvature and decreases as size decreases. This is the phenomenon of melting point depression.[12]

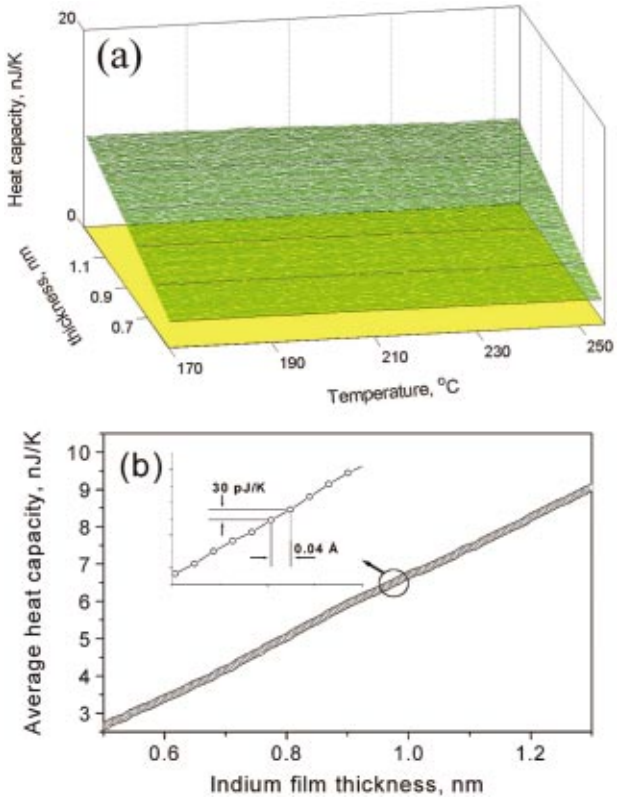

FIG. 2. (Color) (a) Heat capacity of liquid indium (region A in Fig. 1). For each scan the heat capacity is approximately constant. However, as deposition proceeds the heat capacity of the film increases, as does the mass of the indium; (b) temperature averaged heat capacity from (a). The inset shows an expanded region of a small section of the main graph. The spacing between adjacent points is 0.04 Å in thickness and 30 pJ/K in heat capacity, illustrating the ultrafine detail of the technique.

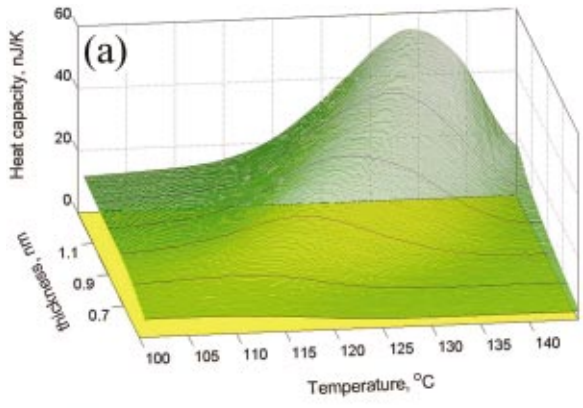

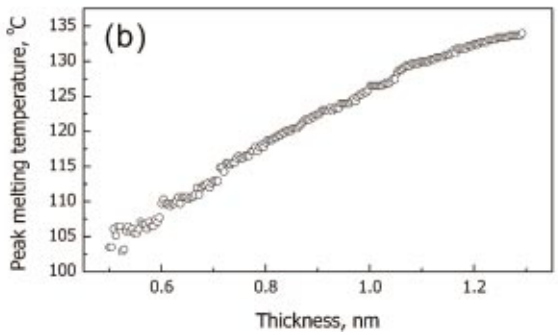

FIG. 3. (Color) (a) Increase of melting temperature during film growth; (b) main melting peak increases continually from 100 to 135 °C as the integrated film thickness increases from 0.5 to 1.3 nm. This shift is due to the increase of average nanoparticle size. This is an example of melting point depression phenomenon.

The peak on each caloric curve represents the endothermic process of melting. The area under the peak is the heat of fusion. One can see in the figure that the melting temperature throughout the deposition is well below the bulk value of indium (156.6 °C). Instead of the sharp melting peak for bulk materials, the caloric curves of thin film indium are extremely broad. As more and more material is deposited onto the surface, the melting peak becomes sharper and shifts towards bulk melting temperature.

We analyze the data by focusing on three main features: (A) the temperature region in which all of the nanoparticles are liquid, (B) the melting peak of the film which illustrates size-dependent melting point depression, and (C) the multiple maxima observed at low temperature (50–90 °C) that are related to the formation of magic number particles.

Heat capacity measurements of liquid indium are shown in Fig. 2(a). Heat capacity is an extensive characteristic of materials. It increases linearly with the mass. One can use the heat capacity to measure the mount of deposited materials. When comparing sequential caloric scans during deposition, the heat capacity of the film systematically increases, as does the mass of the indium. Figure 2(b) is the average value of the heat capacity between 170 and 255 °C as a function of integrated indium thickness. The average is taken over a wide temperature range to increase sensitivity. Due to the melting point depression, only liquid state heat capacity data are available for illustration.

The results show the remarkable sensitivity of the measurement and illustrate the capability for characterizing fine

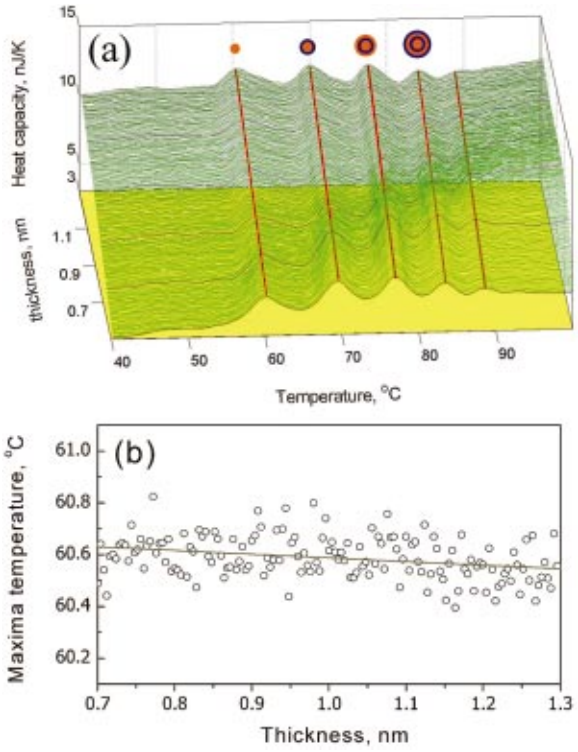

FIG. 4. (Color) At the early stages of deposition, some selected nanoparticles are favored over other sizes due to increased thermodynamic stability. Similar phenomena have also been observed in magic numbers in cluster beams (see Ref. 14) and epitaxial surfaces. (see Ref. 15) As shown in (a) there are multiple maxima in the caloric curve. The maxima temperature correspond to discrete sizes, (see Ref. 13) which is illustrated as schematic inset of nanoparticles with incremental atom layers. Unlike the melting peak shift, shown in Fig. 3, the melting points of selected nanoparticles are relatively constant. This is seen in (b) where the value of the first maxima in (a) remains at 60.0 ± 0.2 °C. The temperature is obtained using a fourth order polynomial fit to the seven data points around the maxima. The ability to observe this high degree of stability is due the reduction of systematic errors by the use of real-time measurements.

details during deposition. Using the technique we can easily resolve film thickness of 0.04 Å and heat capacities of 30 pJ/K.

Caloric data show melting point depression phenomenon [Fig. 3(a)]. This figure illustrates the continuous nature of the melting property change with the mount of material. The width of the melting peak is due to the combination of size distribution and size-dependent melting. For each scan, the smallest particles contribute to the endothermic signal at the beginning (low temperature) of the peak, while the largest ones contribute at the high temperature section of the peak. As deposition proceeds, the overall melting temperature substantially increases as expected since the average size of the clusters also increases. We quantitatively track the overall melting process by obtaining a peak melting temperature of the film, which increases from 100 to 135 °C as the integrated film thickness increases from 0.5 to 1.3 nm shown in Fig. 3(b).

Figure 4 shows the caloric response at low temperature section (region C in Fig. 1). Note the multiple maxima at the low temperatures. This is unexpected since one assumes the size distribution of nanoparticles at the very early stages of deposition should be smooth, and particles are physically similar to each other, thus the caloric response should also be smooth showing one single melting peak. However, a detailed analysis of the position of the multiple maxima[13] indicate that certain size nanoparticles are favored over other sizes. A similar effect has also been observed in magic numbers in cluster beams[14] and epitaxial surfaces.[15] The maxima temperatures correspond to the particle size by a discrete 1 ML difference.[13] Unlike the variation of the main melting peak, which is illustrated in Fig. 3, the melting point of the selected size nanoparticle is relatively constant.

This degree of constancy of the temperature of one single size nanoparticle is difficult to establish using single-shot experiments when comparing one experiment to another. This is because errors in temperature can be due to the differences between sensors, differences in ambient temperature, etc. However, the real-time measurement clearly shows that the positions of these local maxima do remain extremely steady during the thin film growth. The graph in Fig. 4(b) shows that variation in the melting temperature of the example maxima in Fig. 4(a) (60.6 °C) is very small (± 0.2 °C).

In summary, the nanocalorimetry technique is applied for real-time characterizing the thin film growth. The technique is used in generating 3D heat capacity plots that show the continuous property changes of the thin film during deposition. At the early stage indium growth, nanoparticles are formed and show the phenomena of melting point depression and the formation of magic number sized nanoparticles. The resolution of the measurement achieves ~30 pJ/K for heat capacity and 0.04 Å for thickness.

The authors acknowledge P. Infante of the Cornell Nanofabrication Facility for technical support in fabricating calorimetric sensors. The research is supported by NSF 0108694. The calorimetry equipment was developed under NSF 9803019. Microanalysis was performed at the Center of Microanalysis of Materials, MRL, UIUC, supported by U.S. Department of Energy (DEFG02-ER-45439). M.Yu.E. receives partial support from ACS-PRF Contract No. 33580-AC7.

[1] J. A. Mayer and S. S. Lau, *Electronic Materials Science: For Integrated Circuits in Si and GaAs* (Macmillan, New York, 1990).
[2] L. I. Maissel and R. Glang, *Handbook of Thin Film Technology* (McGraw-Hill, New York, 1970).
[3] C. Lu and A. W. Czanderna, *Applications of Piezoelectric Quartz Crystal Microbalances* (Elsevier, Amsterdam, 1984).
[4] S. L. Zhang, F. M. d'Heurle, C. Lavoie, C. Cabral, Jr., and J. M. E. Harper, Appl. Phys. Lett. **73**, 312 (1998).
[5] C. Cabral, Jr., C. Lavoie, J. M. E. Harper, and J. Jordan-Sweet, Thin Solid Films **397**, 194 (2001).
[6] K. F. Peters, J. B. Cohen, and C. Yip-Wah, Phys. Rev. B **57**, 13430 (1998).
[7] G. F. Feng, M. Katiyar, N. Maley, and J. R. Abelson, Appl. Phys. Lett. **59**, 330 (1991).
[8] C. Liu, J. Erdmann, and A. Macrander, Thin Solid Films **355**, 41 (1999).
[9] S. L. Lai *et al.*, Appl. Phys. Lett. **70**, 43 (1997); S. L. Lai, J. R. A. Carlsson, and L. H. Allen, *ibid.* **72**, 1098 (1998); S. L. Lai, J. Y. Guo, V. Petrova, G. Ramanath, and L. H. Allen, Phys. Rev. Lett. **77**, 99 (1996).
[10] E. A. Olson, M. Yu. Efremov, M. Zhang, Z. S. Zhang, and L. H. Allen (unpublished).
[11] K.-N. Tu, J. W. Mayer, and L. C. Feldman, *Electronic Thin Film Science for Electrical Engineers and Materials Scientists* (Macmillian, New York, 1992).
[12] M. Zhang, M. Yu. Efremov, F. Schiettekatte, E. A. Olson, A. T. Kwan, S. L. Lai, T. Wisleder, J. E. Greene, and L. H. Allen, Phys. Rev. B **62**, 10548 (2000).
[13] M. Yu Efremov, F. Schiettekatte, M. Zhang, E. A. Olson, A. T. Kwan, R. S. Berry, and L. H. Allen, Phys. Rev. Lett. **85**, 3560 (2000).
[14] M. Schmidt, R. Kusche, B. von Issendorff, and H. Haberland, Nature (London) **393**, 238 (1998).
[15] S. C. Wang and G. Ehrlich, Surf. Sci. **391**, 89 (1997).